

# RegionPLC: Regional Point-Language Contrastive Learning for Open-World 3D Scene Understanding

Jihan Yang<sup>1\*</sup> Runyu Ding<sup>1\*</sup> Zhe Wang<sup>2</sup> Xiaojuan Qi<sup>1</sup>

<sup>1</sup>The University of Hong Kong <sup>2</sup>SenseTime Research

<https://jihanyang.github.io/projects/RegionPLC>

## Abstract

Existing 3D scene understanding tasks have achieved high performance on close-set benchmarks but fail to handle novel categories in real-world applications. To this end, we propose a **Regional Point-Language Contrastive learning framework**, namely **RegionPLC**, for open-world 3D scene understanding, which equips models trained on closed-set datasets with open-vocabulary recognition capabilities. We propose dense visual prompts to elicit region-level visual-language knowledge from 2D foundation models via captioning, which further allows us to build dense regional point-language associations. Then, we design a point-discriminative contrastive learning objective to enable point-independent learning from captions for dense scene understanding. We conduct extensive experiments on ScanNet, ScanNet200, and nuScenes datasets. Our Region-PLC significantly outperforms previous base-annotated 3D open-world scene understanding approaches by an average of 11.6% and 6.6% for semantic and instance segmentation, respectively. It also shows promising open-world results in absence of any human annotation with low training and inference costs. Code will be released.

## 1. Introduction

3D scene understanding aims to attain a comprehensive semantic knowledge of objects and their surrounding context. While remarkable advancements have been achieved in recognizing closed-set categories on benchmark datasets [12, 35, 26], existing models often fail to identify novel categories beyond the label space of training data. This hinders their practical applicability in real open-world scenarios where objects of novel classes may appear [2, 45]. This motivates us to explore how to equip 3D models trained on closed-set datasets with open-world recognition capabilities, *i.e.* open-world 3D scene understanding.

Most existing works in 3D open-world learning fo-

cus on addressing small-scale object classification problems [46, 49, 17], which yet suffers from high computation costs and performance degradation if extended to open-world scene-level tasks [46, 8]. More recently, an early attempt [8] has been made to extend the 3D model’s open-world recognition capabilities for scene-level tasks through harvesting rich semantic knowledge from vision-language foundation models [28, 36, 44, 1]. Although promising results have been attained, further performance improvements are hindered by its coarse image-level visual input, which is core to distilling language knowledge from vision-language foundation models. As shown in Figure 1, the image-level inputs without prompt [8] only enable the foundation model to identify sparse and salient objects in a scene, such as “car”, “truck” and “street” which is unfavorable for dense open-world scene understanding tasks. This inspires us to inquire into how to generate dense region-level visual prompts to fully unleash the power of 2D foundation models for open-world 3D dense perception tasks.

To this end, we propose a holistic **Regional Point Language Contrastive learning framework**, namely **RegionPLC**, which generates dense region-level visual prompts, captions them using 2D foundation models, and transfer visual-language knowledge to 3D point clouds with point-discriminative contrastive learning. First, we introduce dense sliding windows and object proposals from 2D detection models to generate visual prompts from images and leverage these stimuli to elicit comprehensive semantics from foundation models [36, 48, 24]. Albeit simple, this allows us to obtain fine-grained region-level point language pairs and significantly enriches the vocabulary bank in the open-world scenario (see Figure 1). Second, to better transfer dense visual-language knowledge, we propose a point-discriminative contrastive objective that allows point-wise embeddings to be optimized in a discriminative manner instead of being overwhelmed by nearby unrelated points as in CLIP-style [28] contrastive objective. Such point-discriminative optimization facilitates dense point-wise prediction and open-world understanding with more diverse and semantic-rich point features.

\*equal contribution

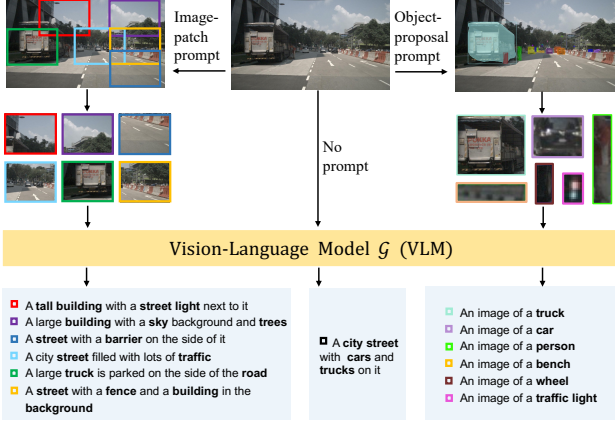


Figure 1. Visualization comparison of view-level captions in PLA [8] and our visual prompted captions on nuScenes [3]. We show sub-sampled sliding window prompted captions and object proposal prompted captions on left and right separately. Instead of focusing only most salient semantics in the whole image as view-level captions [8], our region-level visual prompts elicit more diverse and fine-grained vision-language knowledge from VL foundation models [36, 1, 48, 24]. Best viewed by zooming in.

We conduct extensive experiments on ScanNet [7], ScanNet200 [30], and nuScenes [3] datasets, covering both 3D indoor and outdoor scenarios. Our method outperforms previous state-of-the-art open-world scene understanding method PLA [8] by a large margin: an average of 11.6% gains in terms of unseen category mIoU for semantic segmentation and an average of 6.6% gains in terms of unseen category mAP<sub>50</sub> for instance segmentation. Besides, with only captions from sliding window patches, Region-PLC demonstrates promising zero-shot segmentation performance, lifting 26.1% foreground mIoU compared to PLA [8] that also only leverages task-agnostic language as supervision without any human annotation. It is also noteworthy that without introducing any inference overhead and with only a 6% increase in training costs, Region-PLC can be a lightweight plug-and-play module to inject semantic-rich language supervision into existing state-of-the-art image-feature driven approach OpenScene [27], leading to 2.1% and 5.1% gains on foreground mIoU and mAcc separately.

## 2. Related Work

**3D Scene Understanding.** 3D semantic and instance segmentation are two fundamental perception tasks for scene understanding. Semantic segmentation predicts the semantic meaning of each 3D point cloud, while instance segmentation further differentiates different object instances beyond their semantic categories. For semantic feature extraction and prediction, existing approaches design customized point convolutions applied on raw point clouds [37, 33, 39] or employ sparse convolution [13] to develop voxel-tailored networks [12, 6] or transformers [22] based on 3D grids. For instance prediction, representative approaches typically

use the bottom-up strategy that groups points to form object proposals [20, 35, 34], or first predicts 3D bounding boxes and then refines the object masks using the top-down solution [43, 41, 21]. Though achieving outstanding results on close-set benchmark datasets, they always struggle with open-world recognition, i.e., recognizing novel categories not annotated during training.

**Open-world Learning in 2D.** Open-world understanding aims to recognize unseen classes. Existing popular solution is to train a vision-language foundation model on Internet-scale image-text pairs [31] such as CLIP [28] and ALIGN [19], in order to attain powerful transferable feature extraction ability on even unseen classes. The following works leverage the open-set capacity of these foundation models to enable open-world segmentation [40, 23, 47], detection [14, 29], and other tasks through techniques such as prompting learning [10, 11], module fine-tuning [23, 40], and knowledge distillation [14, 29].

**Open-world Learning in 3D.** Early works in this field follow traditional zero-shot learning setting [5, 25] without accessing language bank or pretrained models, which yield only moderate performance. More recently, 3D open-world learning has been attempted by leveraging 2D foundation models [28, 19] trained on massive multi-modality data. One stream of work [46, 17, 36] explores annotation-free 3D recognition without human annotations via CLIP [28] and extends to scene-level dense prediction relying on additional detection head [49]. However, they incur high inference costs and might inherit 2D prediction failure modes. Recent OpenScene [27] further leverages more powerful 2D open-world segmentation model LSeg [23] and distills knowledge [16] to 3D models, but demands massive memory usage and training overhead. Another stream of work learns on base/seen categories with annotations and extends to novel/unseen categories during inference, which poses challenges in novel class discovery. PLA [8] proposes point-language association by eliciting visual-semantic knowledge encoded in foundation models but still suffers inaccurate dense predictions due to coarse language supervision. In this work, we address both base-annotated and annotation-free scenarios with a unified regional point-language contrastive learning framework. Our method achieves remarkable boosts in 3D open-world scene understanding with relatively low computation overheads. Moreover, it can serve as a lightweight plug-and-play module to combine with existing image-feature driven methods.

## 3. Method

### 3.1. Preliminary

In this work, we target 3D open-world scene understanding. Specifically, during training, the model can assess all points  $\mathcal{P} = \{\mathbf{p}\}$  and human annotation  $\mathcal{Y}$  for base categories  $\mathcal{C}^B$  but cannot access annotations for novel cat-

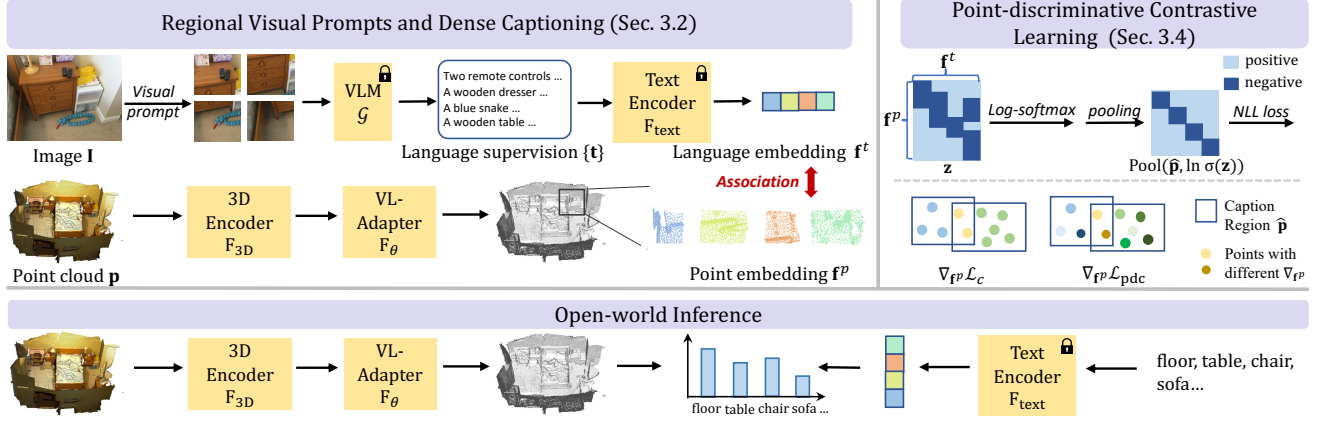


Figure 2. Overview of our regional point-language contrastive learning framework. Regional visual prompts and dense captioning create region-level visual prompts to extract semantic-comprehensive language descriptions  $\mathbf{t}$  from a pretrained visual-language foundation model  $\mathcal{G}$  (see Sec. 3.2). The visual prompts and captions can then be aligned with 3D regions via geometry correspondence to build fine-grained point-language associations (see Sec. 3.3). With point-language pairs, point-discriminative contrastive learning is then used to facilitate point-wise discriminative gradient learning, as opposed to CLIP-style global contrastive objective (see Sec. 3.4). During the open-world inference stage, our approach can infer any classes of interest.

egories  $\mathcal{C}^N$ . During inference, the trained model needs to classify and localize points belonging to both base and novel  $\mathcal{C}^B \cup \mathcal{C}^N$  categories.

To achieve open-world understanding, apart from the common 3D encoder  $F_{3D}$ , we follow [8] to replace the classification layer weights with category embeddings  $\mathbf{f}^l$  extracted from a pretrained text encoder  $F_{\text{text}}$  of CLIP [28]. Hence, the prediction process is shown as follows:

$$\mathbf{f}^p = F_{\theta}(F_{3D}(\mathbf{p})), \mathbf{s} = \sigma(\mathbf{f}^l \cdot \mathbf{f}^p), \mathbf{o} = F_{\text{loc}}(F_{3D}(\mathbf{p}), \mathbf{s}), \quad (1)$$

where  $F_{\theta}$  is the vision-language (VL) adapter to align the feature dimension of the 3D point-wise features  $\mathbf{f}^p$  and category embeddings  $\mathbf{f}^l$ ,  $\mathbf{s}$  is the semantic classification score,  $\sigma$  is the softmax function,  $\mathbf{o}$  is the instance proposal output, and  $F_{\text{loc}}$  is the localization network [35] for instance segmentation. With these modifications, as shown in the bottom part of Figure 2, the model can predict any desired categories by computing similarity between point-wise features and queried category embeddings for open-world inference.

### 3.2. Regional Visual Prompts and Dense Captioning

**Motivation.** Existing state-of-the-art open-world model PLA [8] achieves promising results by distilling language supervisions from 2D image captioning foundation models using images as visual inputs. However, such coarse and sparse image-level captions actually create an easily accessible upper bound for open-world learners with only supervision for the most salient objects in each image. As shown in Figure 1 (middle), the image-level captioning strategy ignores many semantic objects and fails to provide fine-grained language descriptions for plenty of objects. This will definitely penalize dense prediction tasks in open-world scenarios. Additionally, this problem becomes more severe in images with large fields of view such as those in

autonomous driving datasets (see Figure 1 (middle)).

To this end, we propose to explore region-level visual prompts to obtain dense captions from 2D foundation models for precise and accurate language supervision (see the top left of Figure 2). We introduce two region-level visual prompts, *i.e.* image patch via sliding-window and object proposals from 2D detection models, and then extract captions for them from vision-language foundation models [36, 48, 24] (see left and right examples in Figure 1). The two types of visual prompts are orthogonal and can jointly provide dense captions for each scene.

**Image Patch as Visual Prompt.** Without injecting any semantic and objectness priors, regular image patches can naturally become visual prompts for distilling knowledge from foundation models. They can be easily obtained by sliding a window over an image. Besides, sliding windows without category priors actually make vision-language models escape from a pre-defined label space, and thus can discover any potential objectness in the image patch, benefiting the open-world understanding. Specifically, we set a window size  $w_s$  and step size  $w_t$  to generate consecutive image patches  $\mathbf{b}^{\text{sw}}$  in a sliding window manner. By feeding those cropped image patches into an image captioning model  $\mathcal{G}$ , we can obtain dense captions  $\mathbf{t}^{\text{sw}}$  from image patches. We set the step size  $w_t$  to be smaller than the window size  $w_s$  to create overlap between image patches. Hence, those pixels associated with multiple patches/captions can better attain proper dense point-wise supervision by assembling multiple captions. Above process can be illustrated as follows:

$$\mathbf{b}^{\text{sw}} = \text{SW}(\mathbf{I}, w_s, w_t), \quad \mathbf{t}^{\text{sw}} = \mathcal{G}(\mathbf{b}^{\text{sw}}), \quad (2)$$

where  $\mathbf{I}$  is a 2D image and SW indicates the sliding window operation. Despite the simplicity of the sliding window visual prompts, we find that the obtained  $\mathbf{t}^{\text{sw}}$  can effectively

capture semantic meaningful patches on the whole image without any prior. As shown in Figure 1 (left), compared to the limited number of concepts that view-level caption can extract, our  $\mathbf{t}^{\text{sw}}$  provides more diverse semantic concepts that correspond to a specific local image region instead of the whole image. Our experimental results also show that it can largely lift the model’s zero-shot dense prediction performance (see Table 5).

**2D Object Proposal as Visual Prompt.** Although image patches obtained using sliding windows can already provide a considerable amount of dense captions, there are still some drawbacks. On the one hand, the regular image patches cannot accurately locate objects, preventing the model from accurately captioning objects. On the other hand, it is inefficient for the sliding window method to produce dense patches covering objects of various scales, where a massive number of redundant patches are needed. In this regard, we also explore the potential of using object proposals  $\mathbf{b}^{\text{obj}}$  from 2D open-vocabulary object detection models with a pre-defined huge label space such as LVIS [15] to generate visual prompts. These proposals can be used to generate dense captions either by feeding them into a caption foundation model as Eq. (2) or by utilizing the semantic prediction from open-vocabulary object detection models [48, 24, 42] with a language prompt template as CLIP [28] and LSeg [23] does.

**Discussions.** In a nutshell, the two types of visual prompts are complementary. Without injecting objectness/label priors, image patches can cover objects of arbitrary categories, benefiting open-world tasks, which yet sacrifice precise localization. In contrast, 2D object proposals provide more accurate localization of objects, benefiting accurate captioning. However, they might suffer from the open-world capability of the 2D detection model that can only provide proposals of certain categories. The two types of visual prompts will join forces to provide dense language supervision for point cloud representation learning.

### 3.3. Associate Points to Dense Captions

After obtaining regional visual prompts  $\mathbf{b}^r = \mathbf{b}^{\text{sw}} \cup \mathbf{b}^{\text{obj}}$  and regional language  $\mathbf{t}^r = \mathbf{t}^{\text{sw}} \cup \mathbf{t}^{\text{obj}}$ , the next step is to associate them to a partial point set as PLA [8]. Instead of back projecting each RGB-D image to 3D space as PLA [8], we project 3D points onto 2D images to associate points with dense captions. Similar to [27, 4], we project 3D points  $\mathbf{p} \in \mathbb{R}^3$  to obtain its corresponding 2D locations  $\mathbf{u} = (u, v)$  according to projection matrix  $\mathbf{T}$  as follow,

$$[\mathbf{u}, d] = \mathbf{T} [\mathbf{p}, 1], \quad (3)$$

where  $[\cdot, \cdot]$  denotes the concatenation operator and  $\mathbf{T} \in \mathbb{R}^{3 \times 4}$  is the projection matrix combining camera intrinsic matrix and world-to-camera extrinsic matrix. We then obtain valid pixels  $\mathbf{u}^{\text{valid}}$  by filtering occluded pixels or pix-

els outside the image similar to OpenScene [27] and FocalsConv [4] for indoor and outdoor datasets, respectively. Finally, by including only pixels  $\mathbf{u}^{\text{valid}}$  that inside each visual prompt  $\mathbf{b}^r$ , we get the corresponding partial pixel set  $\hat{\mathbf{u}}$  and point set  $\hat{\mathbf{p}}$  leveraging the point to pixel association relation in Eq. (3). Compared to previous view-level point-language learning [8], our regional point-language association enables local and fine-grained partial point set  $\hat{\mathbf{p}}$  to learn from diverse and semantic-rich language supervision.

**View/Entity Association vs Regional Association.** In order to quantitatively comprehend the advantages of the regional point-language association, we compare it with view-level  $\mathbf{t}^v$  and entity-level  $\mathbf{t}^e$  point-caption pairing strategies proposed in PLA [8] with respect to the diversity of language supervision  $\mathbf{t}$  and the coverage of the point set  $\hat{\mathbf{p}}$ . As shown in Table 1, image patch prompted captions  $\mathbf{t}^{\text{sw}}$  provide superior point-language association compared to  $\mathbf{t}^v$  and  $\mathbf{t}^e$  in terms of denser captions in each scene, more diverse concepts for potential objectness, more accurate point set localization (*i.e.* fewer points per  $\mathbf{t}$ ) and a broader point covering ratio. In addition, object proposal prompted captions  $\mathbf{t}^{\text{obj}}$  complement  $\mathbf{t}^{\text{sw}}$  by providing accurate object-wise point-language associations with fewer points per caption and including potentially missed small and distant objects in  $\mathbf{t}^{\text{sw}}$  in terms of the most number of captions per scene.

Metrics	$\mathbf{t}^v$ [8]	$\mathbf{t}^e$ [8]	$\mathbf{t}^{\text{obj}}$	$\mathbf{t}^{\text{sw}}$
# $\mathbf{t}$ Per Scene	16	5	212	142
# Unique Concept	450	270	806	1,496
# Points Per $\mathbf{t}$	24,294	3,933	942	2,479
% Points with $\mathbf{t}$	73%	11%	44%	71%

Table 1. Comparisons among different point-language pairing manners. We use ScanNet frames 25K here.<sup>1</sup>

### 3.4. Point-discriminative Contrastive Learning

**CLIP-style Contrastive Loss.** After obtaining point-language pairs  $\langle \hat{\mathbf{p}}, \mathbf{t} \rangle$ , we can then pull paired point and language features together while pushing unmatched features away through CLIP-style [28] contrastive loss as PLA [8] does. Specifically, the CLIP-style contrastive loss for each point-language pair  $\langle \hat{\mathbf{p}}, \mathbf{t} \rangle$  can be formulated as:

$$\mathcal{L}_c = -\ln \frac{\exp(\mathbf{f}^{\hat{\mathbf{p}}} \cdot \mathbf{f}^{\mathbf{t}} / \tau)}{\sum_{i=1}^{n_t} \exp(\mathbf{f}^{\hat{\mathbf{p}}} \cdot \mathbf{f}_i^{\mathbf{t}} / \tau)}, \quad (4)$$

where  $n_t$  is the number of point-language pairs in a scene and  $\tau$  is a learnable temperature,  $\mathbf{f}^{\mathbf{t}} = \mathbf{F}_{\text{text}}(\mathbf{t})$  is the language feature extracted from the text encoder  $\mathbf{F}_{\text{text}}$ , and  $\mathbf{f}^{\hat{\mathbf{p}}} = \text{Pool}(\hat{\mathbf{p}}, \mathbf{f}^{\mathbf{p}})$  is the average-pooled point feature according to the point set  $\mathbf{f}^{\hat{\mathbf{p}}}$ .

However, CLIP [28] targets learning a global image-level feature for the classification task and neglects the demand of learning point-wise discriminative features in

<sup>1</sup>[https://kaldir.vc.in.tum.de/scannet\\_benchmark/documentation](https://kaldir.vc.in.tum.de/scannet_benchmark/documentation)



dense prediction tasks such as semantic segmentation and instance localization. We theoretically show it by first rewriting Eq. (4) as follows,

$$\hat{\mathbf{z}} = \mathbf{f}^{\hat{\mathbf{p}}} \cdot \mathbf{F}^t, \quad \hat{\mathbf{s}} = \sigma(\hat{\mathbf{z}}, \tau), \quad \mathcal{L}_c = -\mathbf{y}^t \cdot \ln \hat{\mathbf{s}}, \quad (5)$$

where  $\mathbf{F}^t = [\mathbf{f}_1^t, \mathbf{f}_2^t, \dots, \mathbf{f}_{n_t}^t]$  concatenates all caption embeddings in a scene,  $\hat{\mathbf{z}}$  measures the similarity between a pooled point set feature and all caption features,  $\sigma$  is the softmax function with the temperature  $\tau$ ,  $\hat{\mathbf{s}}$  is the probability of associating each language description to the point set  $\hat{\mathbf{p}}$ , and  $\mathbf{y}^t$  is the one-hot label with only one non-zero element at the position corresponding to the paired language position for  $\hat{\mathbf{p}}$ . Thus, the gradient of each point feature  $\mathbf{f}^p$  with respect to the objective  $\mathcal{L}_c$  can be calculated as follows,

$$\nabla_{\mathbf{f}^p} \mathcal{L}_c = \frac{(\mathbf{y}^t - \hat{\mathbf{s}}) \cdot \mathbf{F}^t}{\text{card}(\hat{\mathbf{p}})}, \quad (6)$$

where  $\text{card}(\cdot)$  denotes the cardinality of the point set (*i.e.* number of points). Our theoretical analysis in Eq. (6) demonstrates that the contrastive loss used in the CLIP has the undesired effect of forcing all points within a point set  $\hat{\mathbf{p}}$  to be optimized by the same gradient, violating the goal of learning discriminative representations in dense prediction tasks (see Figure 2 top right). For instance, points in the same point set while belonging to different object categories will also be forced to update in the same way.

**Point-discriminative Contrastive Loss.** Considering the limitation of CLIP-style contrastive loss for dense scene understanding tasks, we propose a point-discriminative contrastive loss  $\mathcal{L}_{\text{pdc}}$  which makes the gradient of each point unique and is determined by its own output features. Specifically, instead of pooling features, we pool logarithm of predicted point-wise probability in  $\hat{\mathbf{p}}$  to calculate the  $\mathcal{L}_{\text{pdc}}$  as:

$$\mathbf{z} = \mathbf{f}^p \cdot \mathbf{F}^t, \quad \mathbf{s} = \sigma(\mathbf{z}), \quad \mathcal{L}_{\text{pdc}} = -\mathbf{y}^t \cdot \text{Pool}(\hat{\mathbf{p}}, \ln \mathbf{s}), \quad (7)$$

$$\nabla_{\mathbf{f}^p} \mathcal{L}_{\text{pdc}} = \frac{(\mathbf{y}^t - \mathbf{s}) \cdot \mathbf{F}^t}{\text{card}(\hat{\mathbf{p}})}, \quad (8)$$

where  $\mathbf{z}$  is the similarity matrix between point-wise features and all caption embeddings, and  $\mathbf{s}$  is the probability matrix of associating each point  $\hat{\mathbf{p}}$  to each caption. As illustrated in Eq. (8), when carrying on contrastive learning with a point-discriminative loss  $\mathcal{L}_{\text{pdc}}$ , the gradient of each point will be related to its similarity to all captions, which is unique. This can also be treated as supervising each point with its all associated language descriptions.

**Analysis on Regional Prompted Language Scenario.** Here, we analyze the behavior of our point-discriminative contrastive loss  $\mathcal{L}_{\text{pdc}}$  when cooperating with dense regional captions  $\mathbf{t}^r$ . As above-proved,  $\mathcal{L}_{\text{pdc}}$  enables each point to learn its semantics independently from captions, resulting in more discriminative representations. Nevertheless, inaccurate captions will have a larger detrimental influence on points optimized by  $\mathcal{L}_{\text{pdc}}$  without averaging gradients from other points in the point set. In such a scenario, as discussed

in Sec. 3.2 and Table 1, our regional point-language pairing strategy tends to provide multiple captions for each point with denser captioning fashion and deliberately overlapped visual prompts in sliding window. By implicitly voting gradients from multiple captions, the final supervision signal should still be robust. Similarly, for points with multiple accurate captions, such implicit ensembling will amplify their gradients and accelerate learning without considering other unrelated points in the same point set. Thus, dense regional point-language pairs can alleviate negative effects from inaccurate captions and advance points with accurate captions, which finally assist learning point-wise discriminative representations with  $\mathcal{L}_{\text{pdc}}$  and benefit precise dense predictions (see Table 7 for experimental supports).

## 4. Experiments

### 4.1. Basic Setups

**Datasets and Validation Settings.** To test the effectiveness of RegionPLC, we evaluate it on three popular datasets: ScanNet [7], ScanNet200 [30] and nuScenes [3]. These datasets cover broad application scenarios, including RGB-D image reconstructed 3D indoor rooms (*i.e.* ScanNet [7] and ScanNet200 [30]) and LiDAR scanned autonomous driving scenes (*i.e.* nuScenes [3]). We validate the open-world capability of our method with different numbers of annotated categories, including **base-annotated open world** (*i.e.* part of categories annotated) and **annotation-free open world** (*i.e.* no category annotated). We evaluate our method’s performance on both semantic segmentation and instance segmentation tasks.

**Category Partition.** For base-annotated open-world experiments, we split categories into base and novel on ScanNet [7] following PLA [8]. As for nuScenes [3], we ignore the “otherflat” class and randomly divide the rest 15 classes into B12/N3 (*i.e.* 12 base classes and 3 novel classes) and B10/N5. For ScanNet200 [30], we randomly split 200 classes to B170/N30 and B150/N50. See Suppl. for details.

**Evaluation Metrics.** For semantic segmentation with base categories, we follow the evaluation protocols of [38, 40, 8] to employ  $\text{mIoU}^{\mathcal{B}}$ ,  $\text{mIoU}^{\mathcal{N}}$  and harmonic mean IoU ( $\text{hIoU}$ ) for evaluating base, novel categories and their harmonic mean separately. Similarly, for instance segmentation, we employ  $\text{mAP}_{50}^{\mathcal{B}}$ ,  $\text{mAP}_{50}^{\mathcal{N}}$  and  $\text{hAP}_{50}$ . As for annotation-free semantic segmentation, we use mean IoU and mean accuracy on foreground classes (*i.e.*  $\text{mIoU}^{\dagger}$  and  $\text{mAcc}^{\dagger}$ ) excluding wall, floor and ceiling for evaluation.

**Implementation Details.** We adopt the sparse-convolution-based UNet as the 3D encoder with CLIP [28] text encoder as the final classifier for 3D semantic segmentation, and SoftGroup [35] for instance segmentation as [8]. We use category prompts to replace ambiguous category names such as “manmade” and “drivable surface” with a list of

Method	ScanNet [7]			nuScenes [3]	
	B15/N4	B12/N7	B10/N9	B12/N3	B10/N5
3DGenZ [25]	20.6 / 56.0 / 12.6	19.8 / 35.5 / 13.3	12.0 / 63.6 / 06.6	01.6 / 53.3 / 00.8	01.9 / 44.6 / 01.0
3DTZSL [5]	10.5 / 36.7 / 06.1	03.8 / 36.6 / 02.0	07.8 / 55.5 / 04.2	01.2 / 21.0 / 00.6	06.4 / 17.1 / 03.9
LSeg-3D [8]	00.0 / 64.4 / 00.0	00.9 / 55.7 / 00.1	01.8 / 68.4 / 00.9	00.6 / 74.4 / 00.3	0.00 / 71.5 / 0.00
PLA w/o t [8]	39.7 / 68.3 / 28.0	24.5 / <b>70.0</b> / 14.8	25.7 / 75.6 / 15.5	25.5 / <b>75.8</b> / 15.4	10.7 / 76.0 / 05.7
PLA [8]	65.3 / 68.3 / 62.4	55.3 / 69.5 / 45.9	53.1 / 76.2 / 40.8	47.7 / 73.4 / 35.4	24.3 / 73.1 / 14.5
RegionPLC	<b>69.9 / 68.4 / 71.5</b>	<b>65.1 / 69.6 / 61.1</b>	<b>58.8 / 76.6 / 47.7</b>	<b>62.0 / 75.8 / 52.4</b>	<b>36.6 / 76.7 / 24.1</b>
Fully-Sup.	73.3 / 68.4 / 79.1	70.6 / 70.0 / 71.8	69.9 / 75.8 / 64.9	73.7 / 76.6 / 71.1	74.8 / 76.8 / 72.8

Table 2. Results for open-world 3D semantic segmentation on ScanNet and nuScenes in terms of hIoU / mIoU<sup>B</sup> / mIoU<sup>N</sup>. PLA w/o t denotes training without language supervision in [8]. Best results are presented in **bold**.

concrete category names when encoding category embeddings. We run all experiments with a batch size of 32 on 8 NVIDIA V100 or A100 (see Suppl. for more details).

## 4.2. Base-annotated Open World

**Comparison Methods.** To show the effectiveness of our method, we compare it to previous base-annotated open-world or zero-shot works. 3DGenZ [25] and 3DTZSL [5] are early works for 3D zero-shot segmentation without leveraging images and 2D foundation models reproduced by [8] in ScanNet. LSeg-3D, is a 3D version LSeg [23] reported by [8]. PLA [8] is our main baseline, the state-of-the-art base-annotated open-world 3D segmentation method using image-level captions and CLIP-style contrastive loss.

Method	ScanNet200 [30]	
	B170/N30	B150/N50
3DGenZ <sup>‡</sup> [25]	02.6 / 15.8 / 01.4	03.3 / 14.1 / 01.9
3DTZSL <sup>‡</sup> [5]	00.9 / 04.0 / 00.5	00.7 / 03.8 / 00.4
LSeg-3D <sup>‡</sup> [8]	01.5 / <b>21.1</b> / 00.8	03.0 / 20.6 / 01.6
PLA (w/o t) <sup>‡</sup> [8]	07.5 / 21.0 / 04.6	06.4 / 21.0 / 03.8
PLA <sup>‡</sup> [8]	11.4 / 20.9 / 07.8	10.1 / 20.9 / 06.6
RegionPLC	<b>15.1 / 20.9 / 11.8</b>	<b>12.5 / 21.8 / 08.8</b>
Fully-Sup.	20.9 / 21.7 / 20.1	20.6 / 22.0 / 19.4

Table 3. Open-world 3D semantic segmentation on ScanNet200 [30] in terms of hIoU / mIoU<sup>B</sup> / mIoU<sup>N</sup>. <sup>‡</sup> indicates results are reproduced by us.

**3D Semantic Segmentation.** As shown in Table 2, compared to the previous state-of-the-art method PLA [8], our method largely lifts the mIoU of unseen categories by 6.9%  $\sim$  17.0% with different numbers of seen categories on ScanNet and nuScenes. Furthermore, when compared to baselines without language supervision, *i.e.* 3DGenZ [25], 3DTZSL [5] and PLA w/o t [8], our method even obtains 18.4%  $\sim$  65.4% performance gains among different partitions and datasets. These significant and consistent improvements across indoor and outdoor scenarios show the effectiveness of our RegionPLC framework.

Furthermore, when scaling up to more long-tail dataset ScanNet200 [30], our method still obtains notable mIoU<sup>N</sup> gains ranging from 2.2% to 3.0% compared to PLA [8] as shown in Table 3. In this regard, our proposed region-level language supervision and point-discriminative contrastive

loss show its potential to address 3D open-world understanding toward real-world scenarios (*i.e.* overwhelmed by complex and long-tail categories).

Method	ScanNet		
	B13/N4	B10/N7	B8/N9
LSeg-3D [23]	05.1 / 57.9 / 02.6	02.0 / 50.7 / 01.0	02.4 / 59.4 / 01.2
PLA (w/o t) [8]	21.0 / <b>59.6</b> / 12.6	11.1 / <b>56.2</b> / 06.2	15.9 / <b>63.2</b> / 09.1
PLA [8]	55.5 / 58.5 / 52.9	31.2 / 54.6 / 21.9	35.9 / 63.1 / 25.1
RegionPLC	<b>56.6</b> / 58.2 / <b>55.0</b>	<b>40.7</b> / 54.7 / <b>32.3</b>	<b>42.3</b> / 61.6 / <b>32.2</b>
Fully-Sup.	64.5 / 59.4 / 70.5	62.5 / 57.6 / 62.0	62.0 / 65.1 / 62.0

Table 4. Results for open-world 3D instance segmentation on ScanNet in terms of hAP<sub>50</sub> / mAP<sub>50</sub><sup>B</sup> / mAP<sub>50</sub><sup>N</sup>.

**3D Instance Segmentation.** As our pipeline provides local language descriptions to fine-grained point sets and encourage points to learn discriminative features, it also benefits instance-level localization task. As shown in Table 4, our method consistently brings 2.1%  $\sim$  10.4% gains compared to the state-of-the-art PLA [8] across three partitions on ScanNet. It is noteworthy that our method obtains more obvious improvements for partitions with fewer base categories (*i.e.* B10/N7 and B8/N9), demonstrating the effectiveness of our RegionPLC in enabling the model to distinguish unseen instances without human annotations.

## 4.3. Annotation-free Open World

Here, we validate our method on a more challenging zero-shot open-world segmentation without any annotation.

**Comparison Methods.** As shown in Table 5, we compare three streams of methods: *i*) Methods that need both pretrained 2D segmentation/detection models and images during inference, including MaskCLIP [47], PointCLIP-Seg [49] that equips PointCLIP with segmentation model as [47], and OpenScene-2D [27]. *ii*) Methods that require pretrained 2D segmentation/detection models in training but no images for inference such as OpenScene-3D. *iii*) Methods that require neither 2D segmentation/detection model nor image in inference, including PLA [8] and our RegionPLC (t<sup>sw</sup> only) that trained only on task-agnostic captions.

We consider the usage of 2D task-specific (*i.e.* segmentation/detection) models and images for inference here since they introduce heavy training or inference overhead for the open-world model. Notice that we reproduce all methods as

Method	Images Infer	Task-specific Model	mIoU <sup>†</sup>	mAcc <sup>†</sup>	Train Hours	Extra Storage	Latency
PointCLIP-Seg <sup>†</sup> [46]	✓	✓	2.1	5.5	-	-	1.7 s
MaskCLIP <sup>†</sup> [47]	✓	✓	23.1	40.9	-	-	1.7 s
OpenScene-2D <sup>†</sup> [27]	✓	✓	<b>58.0</b>	<b>71.0</b>	-	-	106.1 s
OpenScene-3D <sup>†</sup> [27]		✓	57.9	70.7	24.8 h	342 G	0.08 s
OpenScene-3D + RegionPLC (t <sup>sw</sup> only)		✓	<b>60.0</b>	<b>75.8</b>	25.5 h	344 G	0.08 s
PLA <sup>†</sup> [8]			17.7	33.5	11.6 h	1.8 G	0.08 s
RegionPLC (t <sup>sw</sup> only)			<b>43.8</b>	<b>65.6</b>	12.7 h	1.7 G	0.08 s
Fully-Sup.	-	-	75.9	84.8	11.0 h	-	0.08 s

Table 5. Annotation-free open-world 3D semantic segmentation on ScanNet. <sup>†</sup> indicates results are reproduced by us.

their codes are either not publicly available or do not support ScanNet segmentation. The training hours and inference latency in Table 5 are measured with 8 NVIDIA A100 GPUs and a single NVIDIA 2080Ti GPU, respectively.

**3D Semantic Segmentation.** As shown in Table 5, PointCLIP-Seg [46], MaskCLIP [47] and OpenScene-2D [27] suffer from huge latency since they need to feed multi-view images to 2D segmentation models during inference. Among these methods, OpenScene-2D [27] achieves the highest performance owing to the powerful 2D segmentation model LSeg [23] and more multi-view images for training, but its huge inference latency hinders its applicability. In contrast, OpenScene-3D [27] achieves similar performance as OpenScene-2D without heavy latency. However, it requires huge extra storage for storing fused point-wise features from OpenScene-2D. This hinders it from scaling up to large-scale 3D datasets such as Waymo [32] (150K scenes) compared to ScanNet [7] (1.2K scenes). Finally, with fast inference speed, PLA [8] and ours RegionPLC (t<sup>sw</sup> only) also train efficiently requiring only point-language pairs as supervision. However, RegionPLC achieves 26% higher mIoU<sup>†</sup> compared to PLA owing to the regional point-language association and point-discriminative contrastive learning. It is also noteworthy that RegionPLC can function as a lightweight plug-and-play module to assist image-driven methods such as OpenScene [27], leading to 2.1% mIoU<sup>†</sup> and 5.1% mAcc<sup>†</sup> gains without inference cost and just 6% more training time.

OpenScene-3D <sup>†</sup> [27]	PLA [8]	RegionPLC (t <sup>sw</sup> only)	Fully-Sup.
5.9 (10.2)	1.8 (3.1)	<b>6.5 (15.9)</b>	23.9 (32.9)

Table 6. Annotation-free open-world semantic segmentation on ScanNet200 [30] in terms of mIoU<sup>†</sup> (mAcc<sup>†</sup>).

**More Long-tail Scenario.** As shown in Table 6, we validate the open-world methods without demanding images in inference on the more challenging long-tail 3D scene understanding dataset ScanNet200 [30]. Notably, RegionPLC (t<sup>sw</sup> only) itself can surpass OpenScene-3D even in the absence of powerful 2D segmentation models, relying only on point-language pairs. OpenScene is less effective on the ScanNet200 with a large number of fine-grained categories as it relies on a 2D segmentation model that forgets a large number of concepts during fine-tuning on segmen-

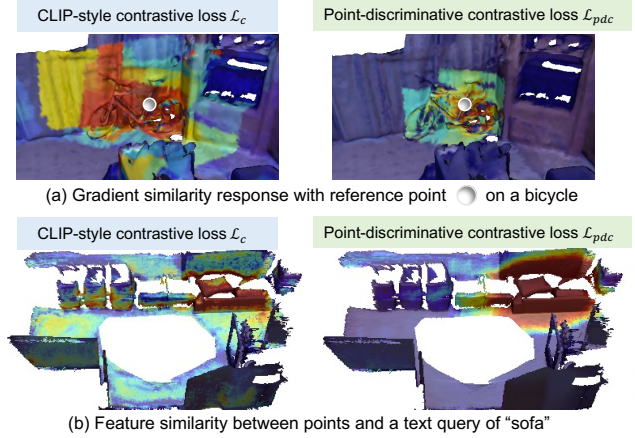


Figure 3. Visualizations of the similarity between gradients and the reference point and between point features and the text embedding of “sofa”. Colors closer to red indicate higher similarity.

tation datasets as verified in [9, 18]. Besides, it may also inherit the shortcomings or bias of the 2D segmentation model. In contrast, our RegionPLC directly learns in a rich vocabulary space with dense and diverse captions which is closer to the open-world scenario.

## 5. Ablation Study

In this section, we examine key components of our framework through in-depth ablation studies. Experimental results for base-annotated and annotation-free open-world experiments are measured in hIoU / mIoU<sup>B</sup> / mIoU<sup>N</sup> and mIoU<sup>†</sup> (mAcc<sup>†</sup>) separately.

Components			ScanNet B15/N4	ScanNet200 B170/N30	ScanNet B0/N19
t <sup>v+e</sup>	t <sup>r</sup>	$\mathcal{L}_{pdc}$	39.7 / 68.3 / 28.0 65.3 / 68.3 / 62.4	07.5 / 21.0 / 04.6 11.4 / 20.9 / 07.8	00.3 (05.3) 17.7 (33.5)
✓			66.3 / <b>68.7</b> / 64.1 67.5 / 68.2 / 66.8	12.8 / 21.1 / 09.2 12.1 / <b>21.3</b> / 08.5	30.8 (54.6) 23.7 (46.9)
	✓	✓	<b>69.9</b> / 68.4 / <b>71.5</b>	<b>15.1</b> / 20.9 / <b>11.8</b>	<b>43.8 (65.6)</b>

Table 7. Component analysis on ScanNet and ScanNet200. t<sup>v+e</sup>, t<sup>r</sup> and  $\mathcal{L}_{pdc}$  denotes the combination of view and entity language supervision [8], our region-level language supervision and our point-discrimination contrastive loss, respectively.

**Component Analysis.** Here, we study the effectiveness of our proposed regional visual prompted captions and point-discriminative contrastive loss. As shown in Table 7, com-



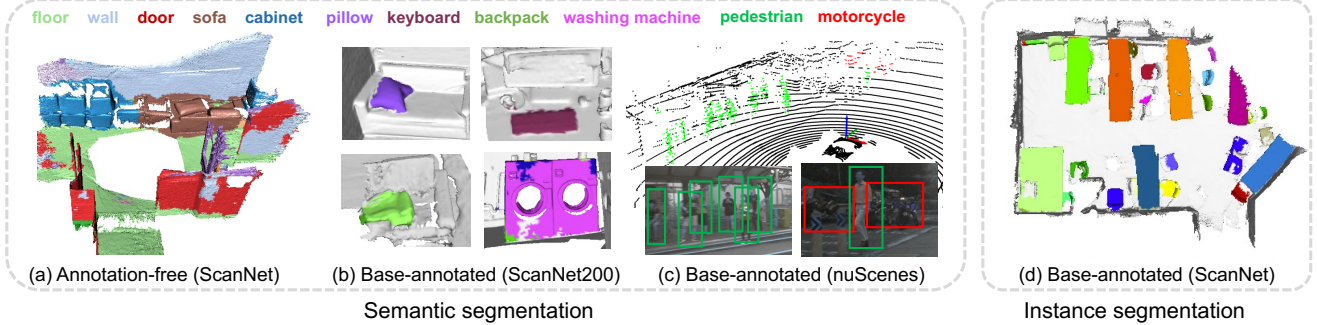


Figure 4. Qualitative results of our RegionPLC. The examples above show annotation-free open-world scene parsing where no human annotation is available (see (a)), and base-annotated open-world learning where a limited number of base classes are annotated (see (b), (c), (d)) for semantic and instance segmentation covering both indoor and outdoor scenarios. Unseen categories are highlighted in colors.

pared to view and entity level captions in PLA [8], our region-level language supervision delivers consistent boosts on three settings. Particularly, it brings 13.1% mIoU<sup>†</sup> gains on ScanNet annotation-free open-world segmentation, demonstrating it consists of rich semantic information for dense scene parsing. Besides,  $\mathcal{L}_{\text{pdc}}$  obtains 2.6%  $\sim$  13.0% gains with region-level captions and 0.7%  $\sim$  6.0% gains with view/entity captions on different settings, illustrating the superiority of learning point-discriminative features. The larger improvement of combining  $\mathcal{L}_{\text{pdc}}$  and  $\mathbf{t}^r$  also verify their synergy effect as analyzed in Sec. 3.4.

ScanNet partition	S3DIS Semantic Segmentation		
	LSeg-3D [8]	PLA [8]	RegionPLC
B15/N4	31.1 (46.6)	39.1 (56.2)	<b>42.4 (56.6)</b>
B12/N7	23.6 (42.7)	35.4 (60.4)	<b>44.7 (63.1)</b>
B10/N9	36.0 (50.9)	43.7 (60.4)	<b>48.6 (63.7)</b>
B0/N19	01.7 (11.2)	13.4 (25.1)	<b>36.9 (53.6)</b>

Table 8. Zero-shot domain transfer results for semantic segmentation in items of mIoU<sup>†</sup> (mAcc<sup>†</sup>) on ScanNet  $\rightarrow$  S3DIS.

**Zero-shot Domain Transfer.** We study the zero-shot domain generalization capability of open-world methods by transferring ScanNet trained model to S3DIS without fine-tuning. As shown in Table 8, RegionPLC enjoys 3.3%  $\sim$  23.5% boosts compared to PLA [8] in mIoU<sup>†</sup> on different splits. Notice that more base categories on ScanNet can hinder the generalization on S3DIS, indicating that dataset-specific annotation penalizes the model’s transferability. In contrast, learning from caption supervision achieves great out-of-domain generalization ability.

**Visualization for Point-discriminative Contrastive Loss.** Here, we provide visualization results on gradients and features to verify the effectiveness of our point-discriminative contrastive loss  $\mathcal{L}_{\text{pdc}}$ . As illustrated in Figure 3 (a), CLIP-style contrastive loss  $\mathcal{L}_c$  will assign the same gradients to unrelated objects and background in the same point set (e.g. large region red points in “bicycle” and “wall” on the left figure), whereas our  $\mathcal{L}_{\text{pdc}}$  generates more discriminative gradients among different points. On the other hand, since  $\mathcal{L}_c$  optimizes the averaged features of a point set, and thus

will assign a high response to unrelated regions. This is shown in Figure 3 (b), where we visualize the feature similarity between each point and a given text query “sofa”.  $\mathcal{L}_c$  produces high responses in massive unrelated regions, while our  $\mathcal{L}_{\text{pdc}}$  assigns the highest response only to the sofa region in the 3D scene. These illustrations validate the point-discriminative characteristics of our proposed  $\mathcal{L}_{\text{pdc}}$ .

## 6. Qualitative Analysis

To demonstrate the open-world capability of our Region-PLC, we provide compelling qualitative results showcasing its capability in recognizing and localizing novel categories in ScanNet, ScanNet200, and nuScenes. As illustrated in Figure 4 (a), RegionPLC successfully identifies unseen categories without any human annotation, demonstrating the quality and richness of our region-level captions and the effectiveness of our point-discriminative learning objective. For base-annotated cases, our model can recognize challenging tail classes such as “backpack” and “keyboard” with precise segmentation results in indoor scenarios (see Figure 4 (b)) and small-scale objects covering only a few points such as “motorcycle” in outdoor scenarios (see Figure 4 (c)). Moreover, RegionPLC also shows a strong localization ability in open-world instance segmentation, accurately grouping novel objects as shown in Figure 4 (d).

## 7. Conclusion

We have presented a holistic regional point-language contrastive learning framework RegionPLC to recognize and localize unseen categories for open-world 3D scene understanding. RegionPLC builds regional point-language pairs by generating regional-level visual prompts which are further used to extract dense and diverse captions from powerful VL foundation models. Furthermore, it learns semantic-rich and point-discriminative features from dense point-language pairs aided by the point-discriminative contrastive objective. Extensive experiments demonstrate that RegionPLC significantly outperforms previous open-world scene understanding methods in both indoor and outdoor



scenarios and shows promising results even in the challenging long-tail or annotation-free zero-shot scenarios.

## References

- [1] Jean-Baptiste Alayrac, Jeff Donahue, Pauline Luc, Antoine Miech, Iain Barr, Yana Hasson, Karel Lenc, Arthur Mensch, Katie Millican, Malcolm Reynolds, et al. Flamingo: a visual language model for few-shot learning. *arXiv preprint arXiv:2204.14198*, 2022. [1](#), [2](#)
- [2] Mariusz Bojarski, Davide Del Testa, Daniel Dworakowski, Bernhard Firner, Beat Flepp, Prasoon Goyal, Lawrence D Jackel, Mathew Monfort, Urs Muller, Jiakai Zhang, et al. End to end learning for self-driving cars. *arXiv preprint arXiv:1604.07316*, 2016. [1](#)
- [3] Holger Caesar, Varun Bankiti, Alex H Lang, Sourabh Vora, Venice Erin Liong, Qiang Xu, Anush Krishnan, Yu Pan, Giancarlo Baldan, and Oscar Beijbom. nuscenes: A multi-modal dataset for autonomous driving. In *Proceedings of the IEEE/CVF conference on computer vision and pattern recognition*, pages 11621–11631, 2020. [2](#), [5](#), [6](#)
- [4] Yukang Chen, Yanwei Li, Xiangyu Zhang, Jian Sun, and Jiaya Jia. Focal sparse convolutional networks for 3d object detection. In *Proceedings of the IEEE/CVF Conference on Computer Vision and Pattern Recognition*, pages 5428–5437, 2022. [4](#)
- [5] Ali Cheraghian, Shafin Rahman, Dylan Campbell, and Lars Petersson. Transductive zero-shot learning for 3d point cloud classification. In *Proceedings of the IEEE/CVF Winter Conference on Applications of Computer Vision*, pages 923–933, 2020. [2](#), [6](#)
- [6] Christopher Choy, JunYoung Gwak, and Silvio Savarese. 4d spatio-temporal convnets: Minkowski convolutional neural networks. In *Proceedings of the IEEE/CVF Conference on Computer Vision and Pattern Recognition*, pages 3075–3084, 2019. [2](#)
- [7] Angela Dai, Angel X Chang, Manolis Savva, Maciej Halber, Thomas Funkhouser, and Matthias Nießner. Scannet: Richly-annotated 3d reconstructions of indoor scenes. In *Proceedings of the IEEE conference on computer vision and pattern recognition*, pages 5828–5839, 2017. [2](#), [5](#), [6](#), [7](#)
- [8] Runyu Ding, Jihan Yang, Chuhui Xue, Wenqing Zhang, Song Bai, and Xiaojuan Qi. Language-driven open-vocabulary 3d scene understanding. *arXiv preprint arXiv:2211.16312*, 2022. [1](#), [2](#), [3](#), [4](#), [5](#), [6](#), [7](#), [8](#)
- [9] Yuxuan Ding, Lingqiao Liu, Chunna Tian, Jingyuan Yang, and Haoxuan Ding. Don’t stop learning: Towards continual learning for the clip model. *arXiv preprint arXiv:2207.09248*, 2022. [7](#)
- [10] Yu Du, Fangyun Wei, Zihe Zhang, Miaojing Shi, Yue Gao, and Guoqi Li. Learning to prompt for open-vocabulary object detection with vision-language model. In *Proceedings of the IEEE/CVF Conference on Computer Vision and Pattern Recognition*, pages 14084–14093, 2022. [2](#)
- [11] Chengjian Feng, Yujie Zhong, Zequn Jie, Xiangxiang Chu, Haibing Ren, Xiaolin Wei, Weidi Xie, and Lin Ma. Promptdet: Towards open-vocabulary detection using uncurated images. 2022. [2](#)
- [12] Benjamin Graham, Martin Engelcke, and Laurens Van Der Maaten. 3d semantic segmentation with submanifold sparse convolutional networks. In *Proceedings of the IEEE conference on computer vision and pattern recognition*, pages 9224–9232, 2018. [1](#), [2](#)
- [13] Benjamin Graham and Laurens van der Maaten. Submanifold sparse convolutional networks. *arXiv preprint arXiv:1706.01307*, 2017. [2](#)
- [14] Xiuye Gu, Tsung-Yi Lin, Weicheng Kuo, and Yin Cui. Open-vocabulary object detection via vision and language knowledge distillation. *arXiv preprint arXiv:2104.13921*, 2021. [2](#)
- [15] Agrim Gupta, Piotr Dollar, and Ross Girshick. Lvis: A dataset for large vocabulary instance segmentation. In *Proceedings of the IEEE/CVF conference on computer vision and pattern recognition*, pages 5356–5364, 2019. [4](#)
- [16] Geoffrey Hinton, Oriol Vinyals, and Jeff Dean. Distilling the knowledge in a neural network. *arXiv preprint arXiv:1503.02531*, 2015. [2](#)
- [17] Tianyu Huang, Bowen Dong, Yunhan Yang, Xiaoshui Huang, Rynson WH Lau, Wanli Ouyang, and Wangmeng Zuo. Clip2point: Transfer clip to point cloud classification with image-depth pre-training. *arXiv preprint arXiv:2210.01055*, 2022. [1](#), [2](#)
- [18] Krishna Murthy Jatavallabhula, Alihusein Kuwajerwala, Qiao Gu, Mohd Omama, Tao Chen, Shuang Li, Ganesh Iyer, Soroush Saryazdi, Nikhil Keetha, Ayush Tewari, et al. Conceptfusion: Open-set multimodal 3d mapping. *arXiv preprint arXiv:2302.07241*, 2023. [7](#)
- [19] Chao Jia, Yinfei Yang, Ye Xia, Yi-Ting Chen, Zarana Parekh, Hieu Pham, Quoc Le, Yun-Hsuan Sung, Zhen Li, and Tom Duerig. Scaling up visual and vision-language representation learning with noisy text supervision. In *International Conference on Machine Learning*, pages 4904–4916. PMLR, 2021. [2](#)
- [20] Li Jiang, Hengshuang Zhao, Shaoshuai Shi, Shu Liu, Chi-Wing Fu, and Jiaya Jia. Pointgroup: Dual-set point grouping for 3d instance segmentation. *Proceedings of the IEEE Conference on Computer Vision and Pattern Recognition (CVPR)*, 2020. [2](#)
- [21] Maksim Kolodiazny, Danila Rukhovich, Anna Vorontsova, and Anton Konushin. Top-down beats bottom-up in 3d instance segmentation. *arXiv preprint arXiv:2302.02871*, 2023. [2](#)
- [22] Xin Lai, Jianhui Liu, Li Jiang, Liwei Wang, Hengshuang Zhao, Shu Liu, Xiaojuan Qi, and Jiaya Jia. Stratified transformer for 3d point cloud segmentation. In *Proceedings of the IEEE/CVF Conference on Computer Vision and Pattern Recognition*, pages 8500–8509, 2022. [2](#)
- [23] Boyi Li, Kilian Q Weinberger, Serge Belongie, Vladlen Koltun, and Rene Ranftl. Language-driven semantic segmentation. In *International Conference on Learning Representations*, 2022. [2](#), [4](#), [6](#), [7](#)
- [24] Liunian Harold Li, Pengchuan Zhang, Haotian Zhang, Jianwei Yang, Chunyuan Li, Yiwu Zhong, Lijuan Wang, Lu Yuan, Lei Zhang, Jenq-Neng Hwang, et al. Grounded language-image pre-training. In *Proceedings of the*

- IEEE/CVF Conference on Computer Vision and Pattern Recognition*, pages 10965–10975, 2022. 1, 2, 3, 4
- [25] Björn Michele, Alexandre Boulch, Gilles Puy, Maxime Bucher, and Renaud Marlet. Generative zero-shot learning for semantic segmentation of 3d point clouds. In *2021 International Conference on 3D Vision (3DV)*, pages 992–1002. IEEE, 2021. 2, 6
- [26] Ishan Misra, Rohit Girdhar, and Armand Joulin. An End-to-End Transformer Model for 3D Object Detection. In *ICCV*, 2021. 1
- [27] Songyou Peng, Kyle Genova, Chiyu Jiang, Andrea Tagliasacchi, Marc Pollefeys, Thomas Funkhouser, et al. Openscene: 3d scene understanding with open vocabularies. *arXiv preprint arXiv:2211.15654*, 2022. 2, 4, 6, 7
- [28] Alec Radford, Jong Wook Kim, Chris Hallacy, Aditya Ramesh, Gabriel Goh, Sandhini Agarwal, Girish Sastry, Amanda Askell, Pamela Mishkin, Jack Clark, et al. Learning transferable visual models from natural language supervision. In *International Conference on Machine Learning*, pages 8748–8763. PMLR, 2021. 1, 2, 3, 4, 5
- [29] Hanoona Rasheed, Muhammad Maaz, Muhammad Uzair Khattak, Salman Khan, and Fahad Shahbaz Khan. Bridging the gap between object and image-level representations for open-vocabulary detection. In *36th Conference on Neural Information Processing Systems (NIPS)*, 2022. 2
- [30] David Rozenberszki, Or Litany, and Angela Dai. Language-grounded indoor 3d semantic segmentation in the wild. In *Computer Vision—ECCV 2022: 17th European Conference, Tel Aviv, Israel, October 23–27, 2022, Proceedings, Part XXXIII*, pages 125–141. Springer, 2022. 2, 5, 6, 7
- [31] Piyush Sharma, Nan Ding, Sebastian Goodman, and Radu Soricut. Conceptual captions: A cleaned, hypernymed, image alt-text dataset for automatic image captioning. In *Proceedings of the 56th Annual Meeting of the Association for Computational Linguistics (Volume 1: Long Papers)*, pages 2556–2565, 2018. 2
- [32] Pei Sun, Henrik Kretschmar, Xerxes Dotiwalla, Aurelien Chouard, Vijaysai Patnaik, Paul Tsui, James Guo, Yin Zhou, Yuning Chai, Benjamin Caine, et al. Scalability in perception for autonomous driving: Waymo open dataset. In *Proceedings of the IEEE/CVF conference on computer vision and pattern recognition*, pages 2446–2454, 2020. 7
- [33] Hugues Thomas, Charles R. Qi, Jean-Emmanuel Deschaud, Beatriz Marcotegui, François Goulette, and Leonidas J. Guibas. Kpconv: Flexible and deformable convolution for point clouds. *Proceedings of the IEEE International Conference on Computer Vision*, 2019. 2
- [34] Thang Vu, Kookhoi Kim, Tung M Luu, Thanh Nguyen, Junyeong Kim, and Chang D Yoo. Softgroup++: Scalable 3d instance segmentation with octree pyramid grouping. *arXiv preprint arXiv:2209.08263*, 2022. 2
- [35] Thang Vu, Kookhoi Kim, Tung M. Luu, Xuan Thanh Nguyen, and Chang D. Yoo. Softgroup for 3d instance segmentation on 3d point clouds. In *CVPR*, 2022. 1, 2, 3, 5
- [36] Peng Wang, An Yang, Rui Men, Junyang Lin, Shuai Bai, Zhikang Li, Jianxin Ma, Chang Zhou, Jingren Zhou, and Hongxia Yang. Ofa: Unifying architectures, tasks, and modalities through a simple sequence-to-sequence learning framework. *CoRR*, abs/2202.03052, 2022. 1, 2, 3
- [37] Wenxuan Wu, Zhongang Qi, and Li Fuxin. Pointconv: Deep convolutional networks on 3d point clouds. In *Proceedings of the IEEE/CVF Conference on computer vision and pattern recognition*, pages 9621–9630, 2019. 2
- [38] Yongqin Xian, Subhabrata Choudhury, Yang He, Bernt Schiele, and Zeynep Akata. Semantic projection network for zero-and few-label semantic segmentation. In *Proceedings of the IEEE/CVF Conference on Computer Vision and Pattern Recognition*, pages 8256–8265, 2019. 5
- [39] Mutian Xu, Runyu Ding, Hengshuang Zhao, and Xiaojuan Qi. Paconv: Position adaptive convolution with dynamic kernel assembling on point clouds. In *Proceedings of the IEEE/CVF Conference on Computer Vision and Pattern Recognition*, pages 3173–3182, 2021. 2
- [40] Mengde Xu, Zheng Zhang, Fangyun Wei, Yutong Lin, Yue Cao, Han Hu, and Xiang Bai. A simple baseline for zero-shot semantic segmentation with pre-trained vision-language model. *arXiv preprint arXiv:2112.14757*, 2021. 2, 5
- [41] Bo Yang, Jianan Wang, Ronald Clark, Qingyong Hu, Sen Wang, Andrew Markham, and Niki Trigoni. Learning object bounding boxes for 3d instance segmentation on point clouds. In *Advances in Neural Information Processing Systems*, pages 6737–6746, 2019. 2
- [42] Lewei Yao, Jianhua Han, Youpeng Wen, Xiaodan Liang, Dan Xu, Wei Zhang, Zhenguo Li, Chunjing Xu, and Hang Xu. Detclip: Dictionary-enriched visual-concept paralleled pre-training for open-world detection. *arXiv preprint arXiv:2209.09407*, 2022. 4
- [43] Li Yi, Wang Zhao, He Wang, Minhyuk Sung, and Leonidas J Guibas. Gspn: Generative shape proposal network for 3d instance segmentation in point cloud. In *Proceedings of the IEEE/CVF Conference on Computer Vision and Pattern Recognition*, pages 3947–3956, 2019. 2
- [44] Lu Yuan, Dongdong Chen, Yi-Ling Chen, Noel Codella, Xiyang Dai, Jianfeng Gao, Houdong Hu, Xuedong Huang, Boxin Li, Chunyuan Li, et al. Florence: A new foundation model for computer vision. *arXiv preprint arXiv:2111.11432*, 2021. 1
- [45] Andy Zeng, Shuran Song, Stefan Welker, Johnny Lee, Alberto Rodriguez, and Thomas Funkhouser. Learning synergies between pushing and grasping with self-supervised deep reinforcement learning. In *2018 IEEE/RSJ International Conference on Intelligent Robots and Systems (IROS)*, pages 4238–4245. IEEE, 2018. 1
- [46] Renrui Zhang, Ziyu Guo, Wei Zhang, Kunchang Li, Xupeng Miao, Bin Cui, Yu Qiao, Peng Gao, and Hongsheng Li. Pointclip: Point cloud understanding by clip. In *Proceedings of the IEEE/CVF Conference on Computer Vision and Pattern Recognition*, pages 8552–8562, 2022. 1, 2, 7
- [47] Chong Zhou, Chen Change Loy, and Bo Dai. Extract free dense labels from clip. In *European Conference on Computer Vision (ECCV)*, 2022. 2, 6, 7
- [48] Xingyi Zhou, Rohit Girdhar, Armand Joulin, Philipp Krähenbühl, and Ishan Misra. Detecting twenty-thousand classes using image-level supervision. In *ECCV*, 2022. 1, 2, 3, 4

- [49] Xiangyang Zhu, Renrui Zhang, Bowei He, Ziyao Zeng, Shanghang Zhang, and Peng Gao. Pointclip v2: Adapting clip for powerful 3d open-world learning. *arXiv preprint arXiv:2211.11682*, 2022. [1](#), [2](#), [6](#)